

Re-Think and Re-Design Graph Neural Networks in Spaces of Continuous Graph Diffusion Functionals

Tingting Dan¹, Jiaqi Ding^{1,2}, Ziquan Wei^{1,2}, Shahar Z Kovalsky³, Minjeong Kim⁴, Won Hwa Kim⁵ and Guorong Wu^{1,2}

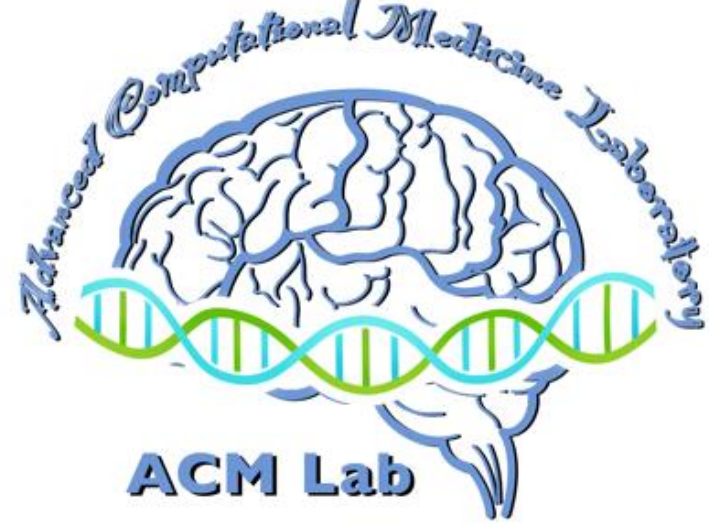
¹ Department of Psychiatry, University of North Carolina at Chapel Hill, NC 27599, USA

² Department of Computer Science, University of North Carolina at Chapel Hill, NC 27599, USA

³ Department of Mathematics, University of North Carolina at Chapel Hill, NC 27599, USA

⁴ Department of Computer Science, University of North Carolina at Greensboro, NC 27402, USA

⁵ Computer Science and Engineering / Graduate School of AI, POSTECH, Pohang, 37673, South Korea



THE UNIVERSITY
of NORTH CAROLINA
at CHAPEL HILL

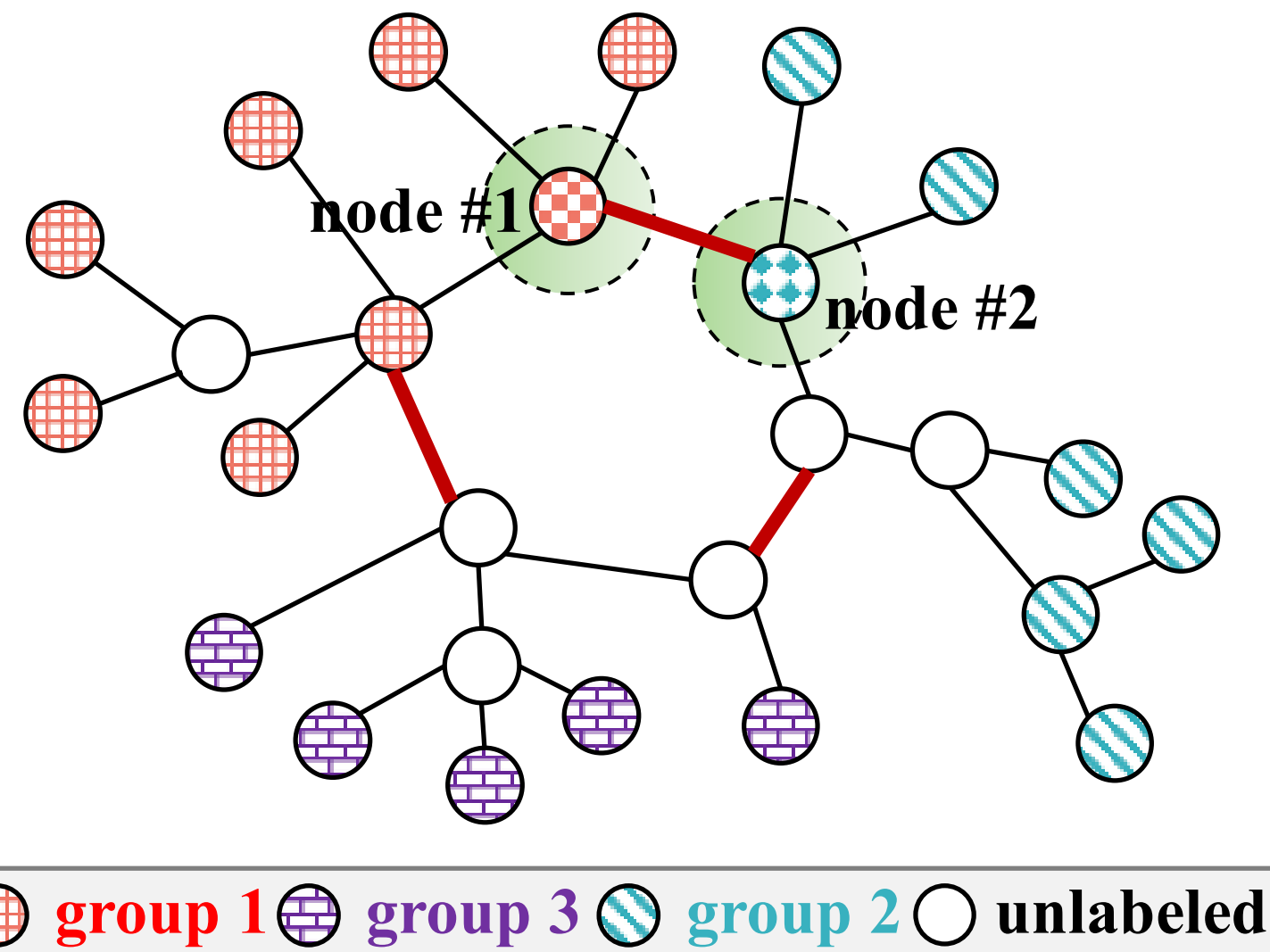
MOTIVATION & OBJECTIVES

METHOD

Motivation: Graphs are ubiquitous in various domains, such as social networks and biological systems. Despite the great successes of graph neural networks (GNNs) in modeling and analyzing complex graph data, the inductive bias of locality assumption, which involves exchanging information only within neighboring connected nodes, restricts GNNs in capturing long-range dependencies and global patterns in graphs.

Challenges: How to devise a new inductive bias for cutting-edge graph application and present a general framework through the lens of variational analysis.

Contribution: In this work, we present the GNN-PDE-COV framework to re-think and re-design GNN models with great mathematical insight. On top of this, we devise the selective inductive bias to address the over-smoothing problem in GNN and develop new GNN model to predict the pathology flows *in-vivo* via longitudinal neuroimages.



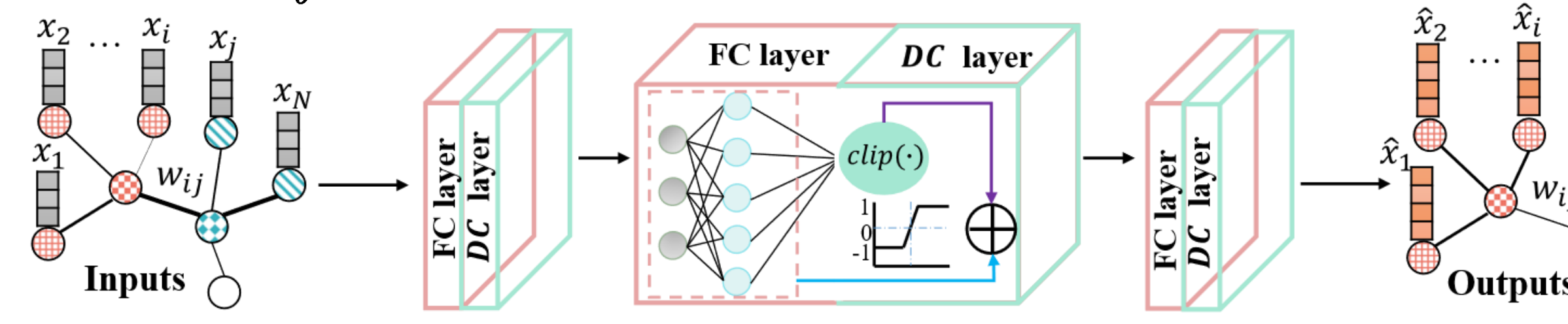
This figure demonstrates the root cause of over-smoothing issue in current GNNs, where node color denotes the group label (no color means unlabeled) and edge thickness indicates connection strength. It is clear that nodes #1 and #2 are located at the boundary of two communities. The inductive bias of GNNs (i.e., locality assumption) enforces the node embedding vectors on node #1 and #2 becoming similar due to being strongly connected (highlighted in red), even though the insight of global topology suggests that their node embeddings should be distinct. Current GNNs only deploy a few layers (typically two or three), which might be insufficient to characterize the complex feature representations on the graph.

Develop VERY deep GNNs with a selective mechanism for link-adaptive inductive bias: We formulate the inductive bias into the functional of graph diffusion pattern, the new objective function is defined as:

$$\mathcal{J}(x, z) = \max_z \min_x \|x - x^0\|_2^2 + \lambda \int (z \nabla g x) dx$$

and it can be refined by:

$$z_i^l = \text{clip} \left(z_i^{l-1} + \frac{2}{\beta \lambda} \nabla g x_i, 1 \right) = \begin{cases} b & |b| \leq 1 \\ 1 & b > 1 \\ -1 & b < -1 \end{cases} \quad \begin{cases} \max_f \frac{df}{dt} = \alpha \otimes \nabla g u \\ \min_u \frac{du}{dt} = \alpha \otimes \text{div}(f) \end{cases}$$



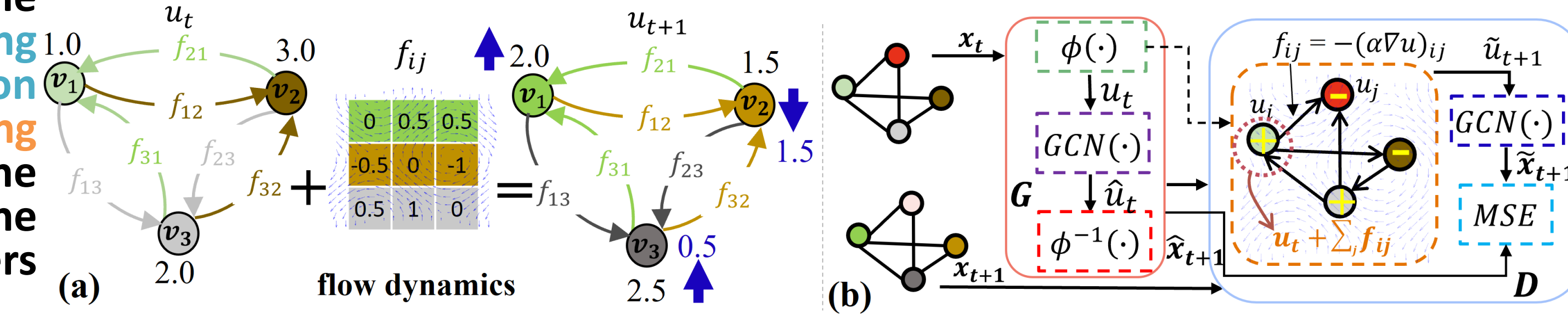
Remarks. The DC layer shifts the diffusion patterns by penalizing the inter-community information exchange (due to strong connections) while remaining the heat-kernel diffusion within the community. The DC layer offers the exact global insight of graph topology to keep the node embeddings distinct between nodes #1 and #2.

Predict flow dynamics through graph neural transport equation: We focus on the conservative system of energy transportation. The system mechanics are formulated as:

$$\frac{dx}{dt} + \text{div}(q) = 0$$

We use Gâteaux variations to optimize $J_{TV}(u, f)$ via the following two coupled time-dependent PDEs

Remarks. We devise a novel GAN model to predict the spreading flows f which not only offers explainability underlying the min-max optimization mechanism in Equation but also sets the stage to understand system dynamics through machine learning.



DATA & RESULTS

Set up: We evaluate the new GNN models derived from our proposed GNN framework in two different applications.

➤ **Experimental results on graph node classification**

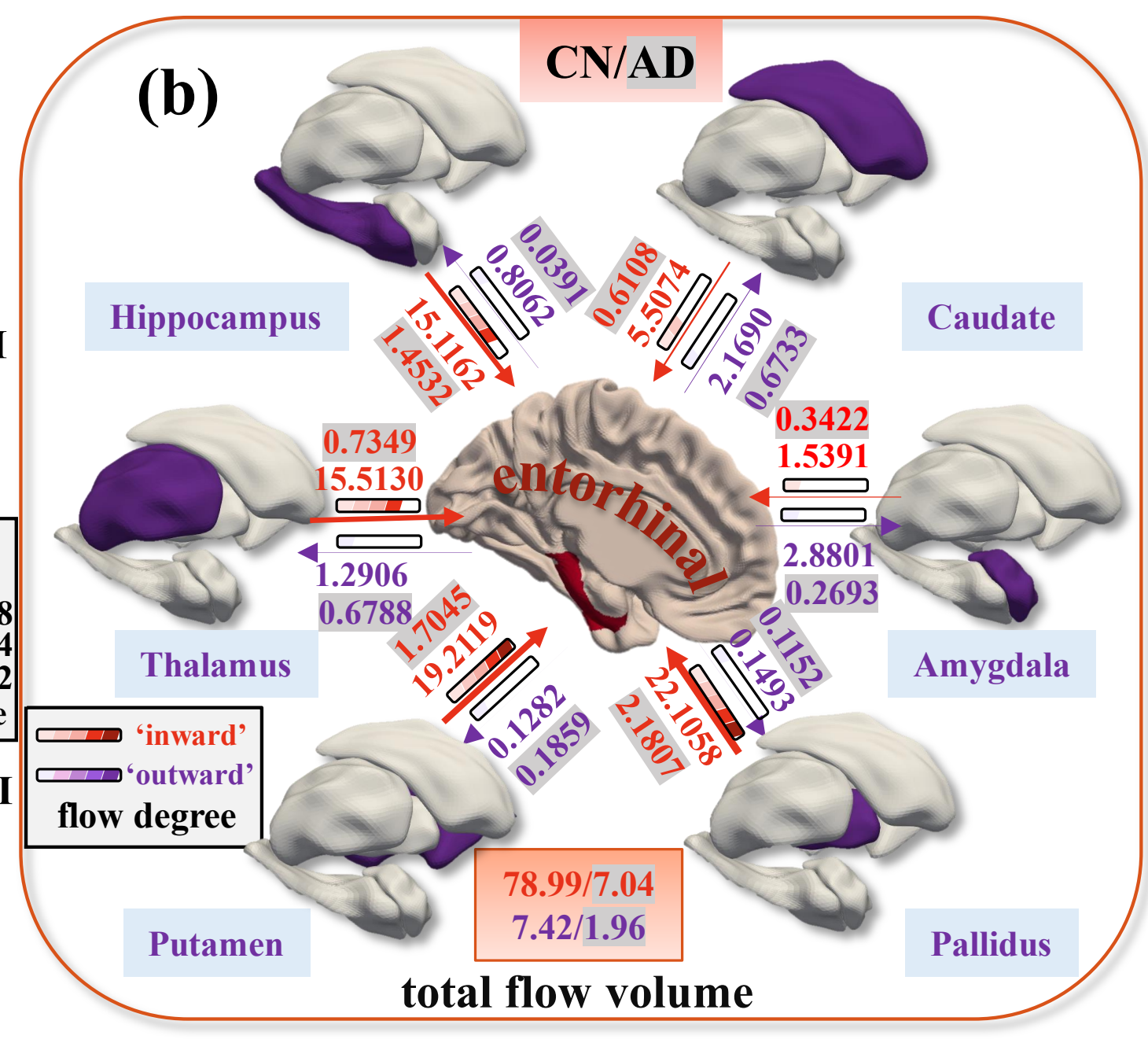
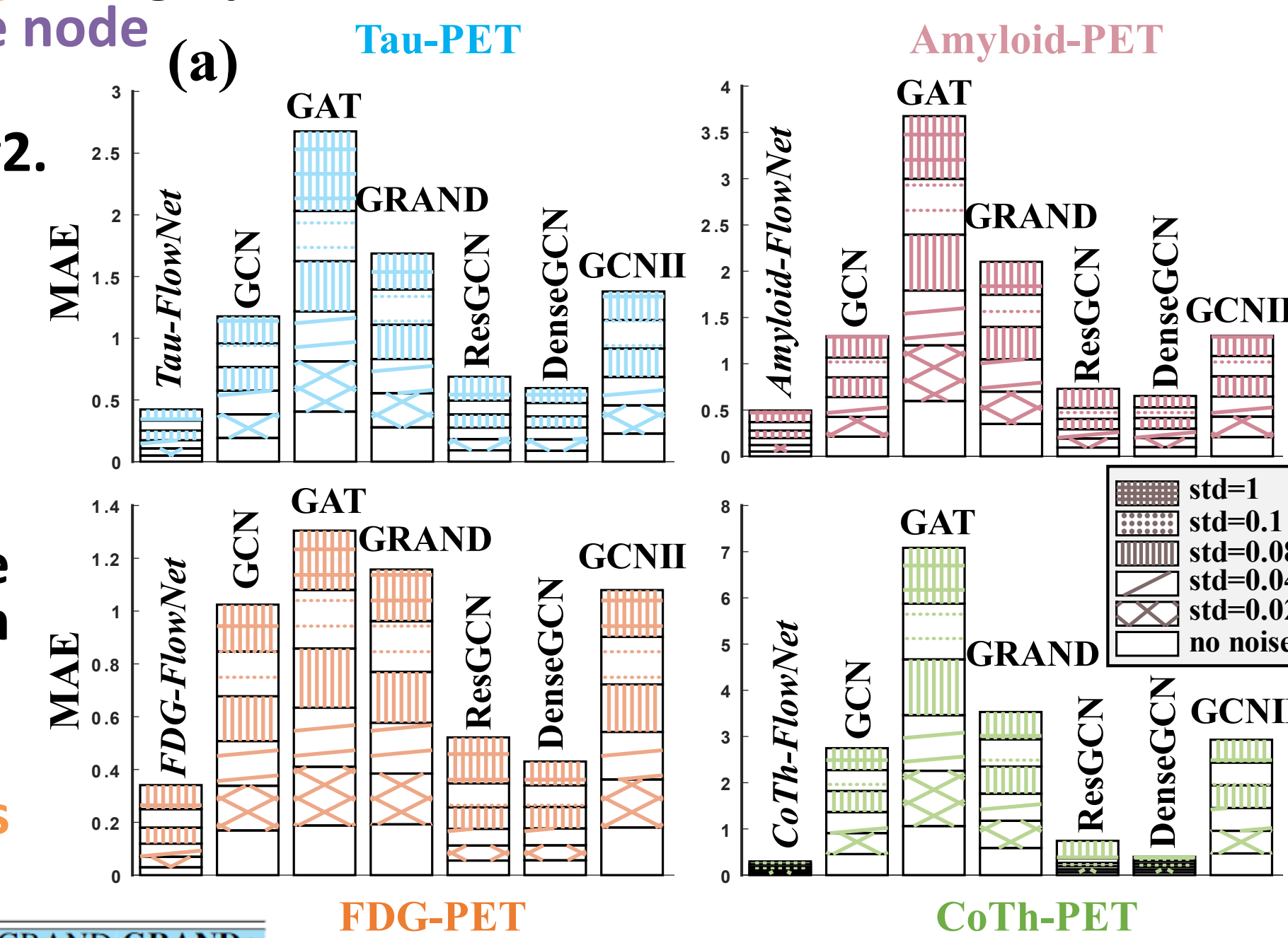
We postulate that by mitigating the over-smoothing issue, we can leverage the depth of GNN models to effectively capture

complex feature representations in graph data.

➤ **Application for uncovering the propagation mechanism of pathological events in AD**

- ❑ We evaluate the prediction accuracy between the ground truth and the estimated concentration values by our X-FlowNet and six GNN methods.
- ❑ We do the potential of disease risk prediction.
- ❑ We examine the spreading flows of tau aggregates in CN (cognitively normal) and AD groups.

Dataset	Model	L=2	L=4	L=8	L=16	L=32	L=64	L=128
Cora	GCN	81.30	79.90	75.70	25.20	20.00	31.80	20.80
	GCN+	82.70 ^{1.40†}	82.70 ^{2.80†}	82.30 ^{6.0†}	70.60 ^{45.4†}	67.80 ^{47.8†}	66.60 ^{34.8†}	59.90 ^{39.1†}
	GAT	82.40	80.30	57.90	31.90	31.90	31.90	31.90
	GAT+	82.60 ^{0.20†}	80.50 ^{0.20†}	69.70 ^{11.8†}	66.00 ^{34.1†}	63.60 ^{63.6†}	54.60 ^{54.6†}	45.70 ^{45.7†}
	GRAND	80.00	82.64	82.74	83.45	81.83	80.81	79.19
	GRAND+	81.93 ^{1.93†}	83.45 ^{0.81†}	82.95 ^{0.20†}	84.27 ^{1.32†}	83.15 ^{0.71†}	81.52 ^{0.71†}	80.10 ^{0.91†}
	ResGCN	76.30	77.30	76.20	77.60	73.30	31.90	31.90
	ResGCN+	77.60 ^{1.50†}	78.70 ^{1.40†}	78.80 ^{2.60†}	78.60 ^{1.00†}	76.90 ^{3.60†}	76.80 ^{44.9†}	33.60 ^{1.70†}
	DenseGCN	76.60	78.50	76.00	76.00	76.00	76.00	76.00
	DenseGCN+	78.00 ^{1.40†}	78.70 ^{0.20†}	76.90 ^{1.40†}	—	—	—	—
Citeseer	GCN	76.40	81.90	81.50	84.80	84.60	85.50	85.30
	GCN+	84.70 ^{8.30†}	84.80 ^{2.90†}	84.70 ^{3.20†}	85.20 ^{0.40†}	85.40 ^{0.80†}	86.30 ^{0.80†}	85.60 ^{0.30†}
	GAT	70.20	62.50	62.90	21.00	17.90	22.90	19.80
	GAT+	72.90 ^{2.70†}	67.30 ^{1.80†}	72.00 ^{1.10†}	54.70 ^{33.7†}	50.30 ^{32.4†}	48.40 ^{25.5†}	46.60 ^{26.8†}
	GRAND	71.94	58.60	26.60	18.10	31.30	30.60	29.30
	GRAND+	72.26 ^{0.32†}	73.55 ^{0.97†}	73.87 ^{0.21†}	47.60 ^{31.3†}	75.16 ^{0.65†}	75.52 ^{0.36†}	74.52 ^{1.62†}
	ResGCN	67.10	66.00	63.60	65.50	62.30	18.80	18.10
	ResGCN+	68.00 ^{0.90†}	67.60 ^{1.60†}	66.00 ^{2.40†}	66.00 ^{0.50†}	65.80 ^{3.50†}	24.00 ^{5.20†}	24.30 ^{6.20†}
	DenseGCN	67.40	64.00	62.20	—	—	—	—
	DenseGCN+	67.80 ^{0.40†}	66.60 ^{2.60†}	64.70 ^{2.50†}	—	—	—	—
Pubmed	GCN	66.50	67.80	69.30	71.60	73.10	71.40	70.20
	GCN+	72.40 ^{5.90†}	73.30 ^{5.5†}	73.80 ^{1.50†}	73.40 ^{1.80†}	73.80 ^{0.70†}	74.60 ^{3.20†}	73.90 ^{3.70†}
	GAT	72.50	77.30	77.30	40.90	38.20	38.10	38.70
	GAT+	79.80 ^{1.30†}	79.10 ^{2.60†}	78.20 ^{0.90†}	77.40 ^{36.5†}	76.20 ^{38.0†}	75.10 ^{37.0†}	73.00 ^{34.3†}
	GRAND	71.94	72.58	73.87	75.00	75.16	72.90	69.52
	GRAND+	72.26 ^{0.32†}	73.55 ^{0.97†}	75.16 ^{1.29†}	75.65 ^{0.65†}	75.52 ^{0.36†}	74.52 ^{1.62†}	72.26 ^{2.74†}
	ResGCN	67.10	66.00	63.60	65.50	62.30	18.80	18.10
	ResGCN+	68.00 ^{0.90†}	67.60 ^{1.60†}	66.00 ^{2.40†}	66.00 ^{0.50†}	65.80 ^{3.50†}	24.00 ^{5.20†}	24.30 ^{6.20†}
	DenseGCN	67.40	64.00	62.20	—	—	—	—
	DenseGCN+	67.80 ^{0.40†}	66.60 ^{2.60†}	64.70 ^{2.50†}	—	—	—	—



Tau	Unit (%)	GCN	GCN+	GAT	GAT+	GCNII	GCNII+	RGCN	RGCN+	DGCN	DGCN+	GRAND	GRAND+
AD/LMCI	Precision	80.15	90.03(*)	69.91	86.18(*)	83.93	90.03(*)	84.64	89.46(*)	84.03	91.58(*)	87.95	88.22(*)
	vs. Accuracy	82.30	88.74(*)	81.05	87.50(*)	83.79	88.75(*)	86.03	90.00(*)	85.54	91.25(*)	88.75	90.12(*)
CN/EMCI	F1-score	75.55	84.49(*)	72.87	84.72(*)	78.82	84.45(*)	83.15	88.54(*)	82.45	91.39(*)	88.14	89.44(*)
AD	Precision	89.29	91.92(*)	87.26	90.13(*)	83.65	88.52(*)	92.61	95.72(*)	92.61	95.91(*)	91.77	95.76(*)
	vs. Accuracy	86.64	90.91(*)	84.86	88.41(*)	76.84	86.36(*)	91.07	95.45(*)	91.07	95.65(*)	90.91	95.45(*)
CN	F1-score	85.64	90.26(*)	83.99	87.16(*)	71.51	84.68(*)	90.45	95.32(*)	90.45	95.55(*)	88.86	95.38(*)

